Available online at www.sciencedirect.com

ScienceDirect

Transportation Research Procedia 29 (2018) 376–389

Transportation Research Procedia

www.elsevier.com/locate/procedia

6th CEAS AIR & SPACE CONFERENCE AEROSPACE EUROPE 2017, CEAS 2017, 16-20 October 2017, Bucharest, Romania

Preliminary weight sizing of light pure-electric and hybrid-electric aircraft

Carlo E.D. Riboldi, Federico Gualdoni, Lorenzo Trainelli*

Politecnico di Milano, Via G. La Masa 34, Milano 20156, Italy

Abstract

The lack of consolidated preliminary design techniques coping with the characteristics of most recent electric and hybrid-electric power plants is often an obstacle for aircraft manufacturers and for owners and operators as well, making the design process less straightforward and hampering comparisons with respect to more traditional designs. In this paper, a technique for the preliminary weight sizing of electric aircraft in the General Aviation category is explained. This is based on existing procedures typical to conventionally-powered aircraft, integrated in a common framework to suitably tackle the issues raised by the peculiar features of electrically-powered aircraft. Then, an expansion of the design method to the case of a series hybrid propulsion system is investigated. Results in virtual environment on a realistic design are also presented.

Peer-review under responsibility of the scientific committee of the 6th CEAS Air & Space Conference Aerospace Europe 2017.

Keywords: electric propulsion; hybrid propulsion; aircraft design procedure; preliminary weight sizing.

1. Introduction

In recent years, the interest of the aviation community for the application of novel propulsion technologies to aircraft of any size has significantly grown. This has been fueled by two main issues encountered with most widespread ICEs (internal combustion engines). Fuel economy is the primary issue for both the owners of smaller private aircraft and for larger airlines, due to the unpredictability of fuel prices and the fact that combustion efficiency appears to be difficult to improve without a major technological breakthrough. Secondarily, noise level close to airports of all sizes is generally still too high. For smaller General Aviation airfields, this results in difficult negotiations with the local communities, often producing heavy traffic limitations which hamper the development of local connections to major airports, and which constitute an obstacle to the development of the always lively field of Sport Aviation (Cohen and Coughlin, 2008). Furthermore, on-board comfort, especially for smaller aircraft, is usually lower due to engine and propeller noise(Miljkovic et al., 2013). For major airlines operating from larger airports noise emissions represent a cost, as most municipalities around larger airports apply fees proportionate to the noise footprint of aircraft operations on the ground (Morrell and Lu, 2000).

Electric and hybrid-electric propulsion may indeed represent an interesting alternative to conventional systems in aviation. The extensive use of electric motors results in a conspicuous noise reduction. Furthermore, the conversion efficiency of electric motors is very high and well above that of ICEs, thus providing a more efficient use of fuel sources.

* Corresponding author. Tel.: +39.02.2399.8387; fax: +39.02.2399.8384.
E-mail address: lorenzo.trainelli@polimi.it

2352-1465
Peer-review under responsibility of the scientific committee of the 6th CEAS Air & Space Conference Aerospace Europe 2017.
10.1016/j.trpro.2018.02.034

Electric and hybrid propulsion are becoming widespread in the automotive field, thanks to the less stringent requirements on weight and reliability typical to this field(Kromer and Heywood, 2007; Pistoia, 2010). Despite its great potential, the application of these propulsion technologies to aviation is still in an embryonic stage. This is due both to technological constraints and community acceptance issues. Battery energy and power densities resulting in excessive weight tolls for an assigned range (Ozawa, 2009), as well as reliability and certification issues bound to the increased number of components, especially for hybrid propulsion systems, are the main technological shortcomings for these new solutions (Cao et al., 2012). For owners and operators, substantial investments would be necessary to design or acquire an aircraft built around a totally new propulsion system, and investment risk would be hard to assess. From a historical perspective, the perception of unusual or novel aircraft configurations by the potential public has been often an obstacle to the success of a new design, thus adding to the investment risk. As a result, electric or hybrid aircraft exist today either as prototypes or as very few models accepted for production that mainly represent conversions of aircraft originally designed for ICE propulsion. All are limited to the light aviation field – thus benefiting from a lower certification burden.

Procedures for the preliminary sizing of ICE-powered aircraft in the general and light aviation categories are well documented in the literature and they are similar under many respects to their counterparts usually adopted for heavier aircraft. On the other hand, few procedures exist for the case of pure-electric or hybrid propulsion (Choi et al., 2005; Pornet et al., 2014; Pornet et al., 2015). The lack of a common design framework is both the origin and the result of the aforementioned issues typical to these propulsion systems. On one side, operational aircraft designed from scratch as pure-electric or hybrid are few, thus making generalization and extrapolation difficult. On the other, the lack of simple procedures of general validity suitable for the preliminary design phase make the first stage of the design of a new model more complicated and costly.

A substantial effort in this sense has been done in a previous publication by Riboldi and Gualdoni (2016), where a general procedure for the preliminary sizing of pure-electric aircraft in the light aviation category has been outlined, without futuristic assumptions on technological levels. Two design examples were presented, one dealing with a semi-acrobatic airplane and the other with a motor-glider. The present paper starts recalling the main results of that work, illustrating the highlights of the preliminary sizing for a pure-electric aircraft and then extending the procedure to a hybrid-electric design. This is based on the evaluation of the effect of the addition of an ICE in a series hybrid configuration, building upon the pure-electric design as a baseline. After recalling the sizing example for the pure-electric motor-glider, the presented method will be applied to a series hybrid-electric version of the same aircraft.

Nomenclature

c_P	brake specific fuel consumption (BSFC)
C_D	drag coefficient
C_L	lift coefficient
e	energy density parameter
E	energy
g	gravity field intensity
k	induced drag coefficient
K_h	design power ratio for ICE
L	length of run
p	power density parameter
P	power
R	cruising range
S	reference wing surface
t	time
V	airspeed
V_v	vertical speed (or rate of climb)
W	weight
η	efficiency
ξ	power loss exponent
ρ	air density

Subscripts

0	total
bat	battery
C	battery recharge
DB	database
e	empty
f	fuel
in	initial

ICE	internal combustion engine
m	electric motor
p	propeller
pl	payload
req	required
$stall$	stall condition
to	take-off

2. Preliminary sizing procedure for a conventional aircraft

2.1. Weight breakdown and historical regression

In preliminary sizing of a propeller-driven aircraft, the design values for the quantities (W_{to}, S, P) are sought, where W_{to} is the design takeoff weight, S is the reference wing surface, and P is the installed power (Roskam, 2003). For conventionally-powered aircraft, either reciprocating engine or turbo-engine powered, the identification of W_{to} starts from the definition of the contributing weight components. Indeed, the breakdown of design takeoff weight comes in the form

$$W_{to} = W_e + W_{pl} + W_f, \tag{1}$$

where W_e is the operational empty weight, W_{pl} is the payload weight, and W_f is fuel weight. In the preceding equation, W_{pl} is known from mission specifications, whileW_e and W_f are unknown. The determination of W_{to} is typically carried out by matching two relations.The first is derived by historical trends referred to the aircraft category of interest, which relates the empty weight to the design take-off weight,

$$W_e = f_1(W_{to}). \tag{2}$$

The second is found by applying the 'fuel fraction method' approach to each mission profile of interest. Fuel fractions are the ratios of final to initial weight of the aircraft for each phase of a given mission profile. A value for the fuel fraction corresponding to each phase of the flight can be found from a statistical analysis applied to short phases like take-off and landing, and from basic flight mechanics analysis for the longer ones, typically cruise and loiter. Assuming a null value of remaining fuel at the end of the mission, the product of all fuel fractions end in the ratio of W_f on W_{to}. Choosing the most demanding among the mission profiles of interest, one obtains a relation

$$\frac{W_f}{W_{to}} = g(W_{to}), \tag{3}$$

which, given that Eq. 1 yields $W_f = W_{to} - (W_e + W_{pl})$, can be recast in terms of W_e as

$$W_e = f_2(W_{to}). \tag{4}$$

Solving the system formed byEqs. 2 and 4, one gets the design values for W_{to} and W_e, complying simultaneously with the possibilities of the available production technology (represented by Eq. 2) and the fuel requirements of the sizing mission profile (represented by Eq. 4).

A second phase allowing to find the values for (S, P) is based on the use of the sizing matrix plot (SMP), also called 'matching plot', in which all performance specifications are considered as functions of design wing loading W_{to}/S and design power loading W_{to}/P. The determination of a candidate pair $(W_{to}/S\,, W_{to}/P)$ through the SMP leads, once W_{to} is known, to the determination of (S, P).

3. Preliminary sizing procedure for small electric aircraft

3.1. Weight breakdown and historical regression

As seen above, in the classical method just sketched, the main ingredients are the empty weight historical regression, the fuel fraction method, and the SMP. For a purely-electric aircraft, for which the fuel fraction method is not applicable, a modification is sought hereafter by integrating the two remaining ingredients. In this case, the breakdown of takeoff weight comes in the form

$$W_{to} = W_e + W_{pl} + W_{bat} + W_m \tag{5}$$

where W_{pl} is the weight of payload, W_{bat} that of the batteries and W_m that of the electric motor, while W_e now represents the operational empty weight without the electric motor. This approach is motivated by the necessity to look for historical data

related to the electric motor, which cannot be derived from the wealth of information related to current and past conventionally-powered aircraft models. Indeed, concerning existing electric aircraft, it is possible to find just a few designs for which reliable values can be obtained. Similarly to the more usual case of ICE-powered aircraft, it is possible to match the historical W_{to} and W_e weight values with a linear regression in the usual bi-logarithmic form (Roskam, 2003),

$$\log(W_{to}) = A + B\log(W_e), \tag{6}$$

leading to an equation of the form seen in Eq. 2. As shown in Fig. 1, the resulting regression matches the experimental data with acceptable accuracy, in relation to the database considered in Riboldi and Gualdoni (2016).

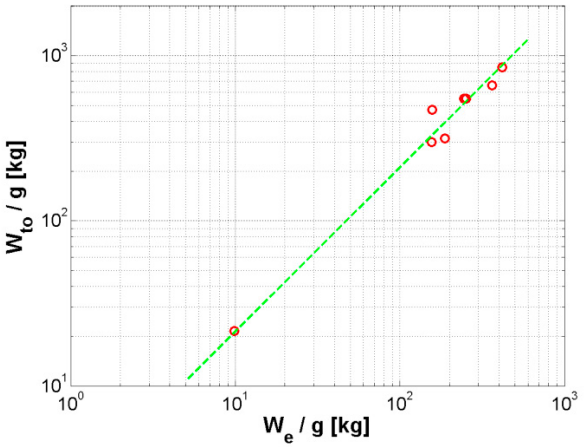

Fig. 1. Real weight data and statistical regression for the considered database.

At this point, the case of an electric aircraft is radically different from a conventional one, due to the fact that an equation in the form of Eq. 4 cannot be derived from the fuel fraction method. Indeed, fuel fractions cannot be defined anymore, for in this case the weight of the aircraft does not change during the flight – meaning also that takeoff weight W_{to} corresponds to the aircraft weight for all phases of the flight. As a consequence, the weight of the battery W_{bat}, which for an electric aircraft has the same conceptual meaning as the weight of fuel for ICE-powered aircraft – *i.e.* the weight of the energy source –, cannot be excluded from Eq. 1.

3.2. Analysis of the mission profile

This major difference can be dealt with starting again from an analysis of the mission profile, studying the effect on weight of the specifications for each phase appearing in it. A very straightforward mission profile will be assumed, that suits the typical flight profile of sport as well as commercial aircraft. It will be composed of five phases: take off, climb, cruise, loiter and landing. Battery weight is affected by two requirements, namely power and energy. The total value of energy to be stored is reflected in a certain amount of battery mass, through an energy density parameter e_{bat} which can be safely assumed in the range of e_{bat}= 130–150 Wh/kg at the current level of technology. The energy requirement can be obtained integrating in time the power requirement for each phase of the flight. As explained in Riboldi and Gualdoni (2016), power can be computed starting from an analysis of the flight mechanics of each flight phase. The general relationship

$$P_{req} = V_v\, W_{to} + \tfrac{1}{2}\rho\, V^2 S\, C_D \tag{7}$$

can be assumed for climb, cruise and loiter, where P_{req} is power required, V true airspeed, V_v vertical speed (or rate of climb), ρ air density, S wing surface, and C_D drag coefficient. The value of the drag coefficient C_D in Eq. 7 will be defined substituting the usual parabolic polar formula $C_D = C_{D0} + kC_L^2$, for which the coefficients C_{D0} and k need to be known. The lift coefficient C_L will be obtained from vertical equilibrium, thus bringing in also the value of W_{to}^2 as follows

$$P_{req} = V_v\, W_{to} + \tfrac{1}{2}\rho\, V^2 S\, C_{D0} + \frac{k\, W_{to}^2}{\frac{1}{2}\rho\, V\, S}. \tag{8}$$

For cruise and loiter the value of V_v in Eq. 8 will be null, whereas it will be usually assigned as a requirement for climb. Air density ρ can be assigned for cruise and loiter, and set to an assumed average constant value for climb.

It should be remarked that for each phase of the flight the power value P_{req} in Eq. 8 is constant, thanks to the fact that W_{to} is constant, hence the corresponding energy value E can be easily computed multiplying power by the duration of the flight phase,

in turn obtained from specifications starting from horizontal or vertical distance and speed for climb and cruise respectively, or directly assigned for loiter.

As pointed out before, besides the energy requirement impacting on battery weight, required power may constitute a constraint, which can be quantified from the figure of power density p_{bat} typical to the adopted batteries. A reasonable value for this quantity may be in the range p_{bat}= 800–900 W/kg.

As a remark, as suggested inRiboldi and Gualdoni (2016), it is possible to neglect the explicit computation of the contributions to energy and power of takeoff and landing. The effect on the sizing of batteries pertaining to these phases will be lower than 1% of the total, and a corresponding safety margin of 1.02 can be applied on the values of energy and power required resulting from the analysis of the other phases.

It can be noted that the wing reference surface S is the only unknown in the weight sizing problem at this stage. Furthermore, it can be noticed that it is possible to rearrange Eq. 8 in terms of the ratios $\frac{W_{to}}{S}$ and $\frac{W_{to}}{P_{req}}$. As explained in Riboldi and Gualdoni (2016), this suggests that, in order to close the problem of weight sizing for a purely electric aircraft, it may be possible to link the analysis of the SMP, which is expressed in terms of these ratios, to that of the mission profile and historical regression just treated. For usual ICE-powered aircraft, finding W_{to} and W_e and the analysis of the SMP are basically independent sections of the design process. For an electric aircraft considering both design tools together constitutes an integrated design approach representing a straightforward way to close the weight sizing problem.

3.3. Analysis of the sizing matrix plot

The sizing matrix plot can be used to put together several constraints in the design phase, arising mainly from desired performance in all phases of the mission, *i.e.* stemming from an analysis of the mission profile, and from applicable certification and other regulations as well. The space of solutions is henceforth limited, and a design point satisfying all limits with a reasonable safety margin can be determined in terms of the ratios $\frac{W_{to}}{S}$ and $\frac{W_{to}}{P_{req}}$, namely wing loading and power loading, see Raymer (2012).

For the aircraft category of interest here, standard rules for the SMP may be those of FAR Part 23 or EASA CS-23. Seven constraints should be considered, namely take-off distance, landing distance, minimum rate of climb in take-off and landing configuration, rate of climb at a specified speed, cruise and loiter airspeeds. The analytic expressions of such constraints are the same for electric aircraft and conventional aircraft, hence they can be found in the literature for those coming from certification procedures, or by manipulation of the equations for the mission profile provided above. The curves corresponding to each constraint can be plot on the plane $\frac{W_{to}}{S}$ and $\frac{W_{to}}{P_{req}}$.

Some requirements for the aircraft need to be guessed in order to set some parameters in the equations of the constraints. For take-off, the ground run distance needs to be assigned. For climb in take-off and landing configurations the respective polar curves of the aircraft must be assigned, and they can be obtained at this stage using the procedure proposed by Roskam(2003). For the constraint represented by cruise speed, it is necessary to know V^{cruise}. For the constraints coming from the mission profile, the clean polar, climb, cruise and loiter speeds, and the vertical speed V_v^{climb} during climb need to be assigned. Furthermore, altitudes for all maneuvers need to be guessed.

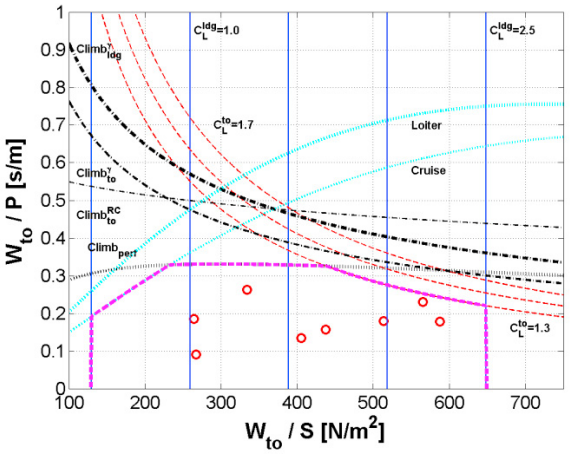

Fig. 2. Sizing matrix plot for the considered motor-glider.

Figure 2 presents a possible SMP for a prototypal mission for which the constraints have been specified based on the investigation of the characteristics of the aircraft in the database. The data refer to a hypothetical motor-glider design, for which the design will be developed further in the following paragraphs. For this case the take-off ground run distance has been set to

200 m at sea level, and cruising and loiter altitude has been set to 1,500 m. Polar coefficients have been obtained imposing an aspect ratio of 30 and a certain level of cleanliness of the aerodynamic construction, that is typical to gliders or lightly powered aircraft. Furthermore, no retractable landing gear have been assumed, and no deployment of flaps on take-off, that is typical of smaller aircraft. For landing, stall speed has been set to $V_{stall}^{landing}$= 40 kn at sea level. Some curves in Fig. 2 are parameterized, in particular for different values of $C_{L,max}$ for the landing constraint and for various C_L^{to} for take-off. Climb, cruise and loiter speeds V^{climb}= 48 kn, V^{cruise}= 90 kn and V^{loiter}= 81 kn respectively are assigned for the corresponding flight phases. Further quantities assigned are the vertical speed in climb in clean configuration, V_v^{climb}= 400 ft/min and the average density during climb.

The curves representing the constraints on the SMP define an area of compliance with respect to all constraints. With the information available at this stage, a possible rule for choosing a design point on the SMP is that of maximizing wing loading, thus reducing the size of the reference surface, and hence of the aircraft, for a given W_{to}. Secondarily, it is possible to set power loading to the highest possible value, in order to assure the lowest power required with respect to a same take-off weight, hence reducing motor weight and cost.

3.4. Choice of the design point and weight sizing via integrated analysis

As explained above, in order to close the problem of finding W_{to} and W_e it is possible to specify a value of $\frac{W_{to}}{S}$, providing a way to explicitly write the equations for the mission profile and computing W_{bat}. Such value can be obtained from the analysis of the SMP, so that all constraints on the plot be implicitly satisfied in terms of wing loading. In practice, the assigned value of wing loading can be used to find the value of the reference wing area $S = W_{to}/\frac{W_{to}}{S}$, thus allowing to compute power required for a given W_{to} through the power equations of the mission profile (Eq. 8). This in turn allows to quantify the energy needed for each part of the mission.

Finally, W_{bat} can be computed as

$$W_{bat} = \frac{g}{\eta_p} max\left\{\frac{E^{climb}+E^{cruise}+E^{loiter}}{e},\ \frac{max\left\{P_r^{climb},\ P_r^{cruise},\ P_r^{loiter},\ W_{to}/\frac{W_{to}}{P}\right\}}{p}\right\} \tag{9}$$

where the maximum between the weight corresponding to the total energy needed for the flight and that obtained from the peak power to be provided to the motor is chosen for the design. Here η_p represents the efficiency of the propeller. Concerning power requirements, it is noteworthy that, besides the constraints coming from the mission profile, the explicit presence of $W_{to}/\frac{W_{to}}{P}$ allows to take into account requirements coming from standard rules or other constraints evidenced in the mission profile. To clarify this point, in case the most stringent requirements on $\frac{W_{to}}{P}$ – leading the choice design point – came from the mission profile, then the presence of $W_{to}/\frac{W_{to}}{P}$ in Eq.9 would not have any visible results.

As a remark, it should be evidenced that, following the choice of the design point in terms of $\frac{W_{to}}{S}$ and $\frac{W_{to}}{P_{req}}$ on the SMP, a value of W_{bat} and hence of W_e can be obtained for every value ofW_{to}. Also, another historical regression for the weight of the electric motor as a function of its power can be established (Riboldi and Gualdoni, 2016), so that a value of *P* and hence of W_m can be obtained for every value of W_{to}.

This in turn allows to close the sizing problem in terms of choice of W_{to} and W_e, by flanking the historical regression in Eq. 6 with a new relationshipderived by Eq. 5, which yields $W_f = W_{to} - \left(W_{pl} + W_{bat} + W_m\right)$, *i.e.* an equation in the form of Eq. 4. Therefore, we get a well-posed system of two equations where, similarly to the case of conventional propulsion, the unknowns are W_{to} and W_e.

The whole procedure can be summarized through the scheme presented in Fig. 3. In particular, it should be noticed that there are two main operational blocks – in dark blue in the figure – , one representing the SMP and producing design wing loading and power loading values, the other representing the explicit weight sizing procedure, resulting in design values for all weights in Eq. 5. The equations for the mission profile are present in both main blocks, providing constraints on the SMP and on one of the sub-procedures in the weight sizing block. The latter is centered on assembling the general definition of weights for an electric aircraft (Eq. 5), which is possible computing the battery weight and motor weight from the requirements of the mission profile.

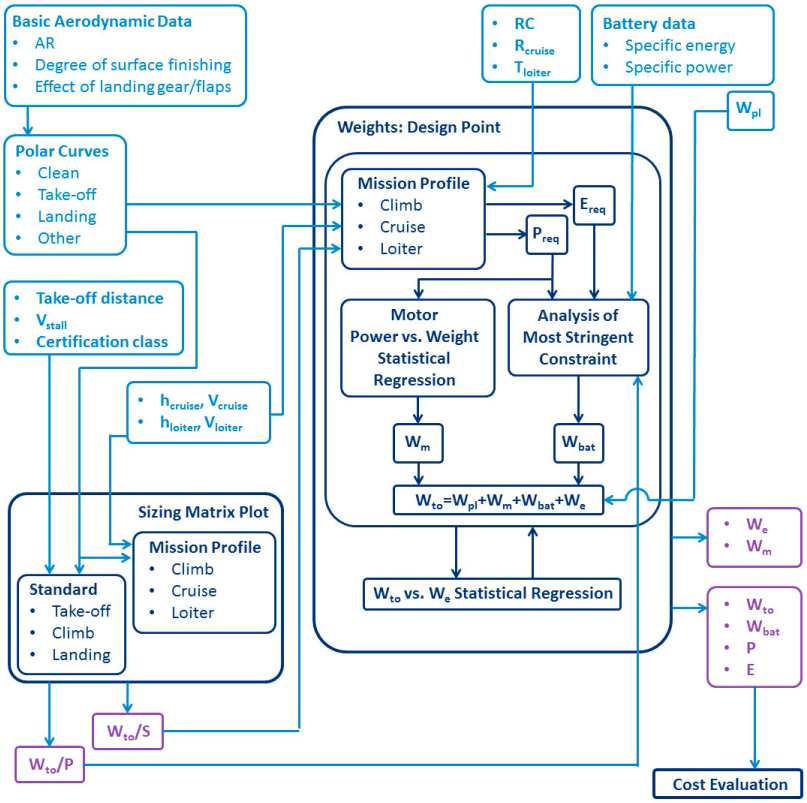

Fig. 3. Integrated preliminary design workflow.

A system of two equations in the unknowns W_{to} and W_e is setup next, composed of the weight definition (Eq. 5) and of the historical regression of W_{to} and W_e data from the database (Eq. 6).

4. Extending the design procedure to hybrid propulsion

Starting from the fully electric design obtained from the integrated design procedure presented above, it is possible to explore the effect on performance attainable by switching to hybrid propulsion. Considering a hybrid propulsion system implies a change to the weight definition in Eq. 5, where the new weights W_{ICE} and W_f, corresponding to the internal combustion engine and stored fuel, are included. For simplicity, a series hybrid propulsion system is hypothesized. In this configuration the internal combustion engine is used to charge the battery, whereas mechanical energy for propulsion is obtained from the same electric motor already sized up in the previous sections.

The key measure of performance considered when studying the effect of the inclusion of a hybrid component in a fully electric propulsion system is cruising range R. This choice can be justified a posteriori, looking at the marked effect the new component of the propulsion system has on this quantity.

In order for the results already obtained to remain valid and to the aim of easing comparisons, it is supposed here to keep a balance between W_{bat} already obtained from the sizing procedure in the case of a pure electric aircraft and the values of the new weight components just introduced. In particular, considering cruise, it is assumed that the part of the weight of the battery necessary for covering cruise, W_{bat}^{cruise}, in the electric design can be split as

$$W_{bat}^{cruise} = W_{bat}^{*} + W_{ICE} + W_f \tag{10}$$

where the component W_{bat}^{*} represents a new battery weight value, reduced with respect to W_{bat}^{cruise} on account of the fact that an internal combustion engine system plus a fuel tank have been now included in the design of the propulsion system. Cruising range R can be computed as a function of two design parameters, namely battery weight W_{bat}^{*} and the power of the installed ICE engine P_{ICE}. Similarly to the electric motor, for which a relationship exists between motor power and weight W_m, also for the ICE case a similar relationship between weight and power can be assumed. In this study a database of engines was built based of smaller marine engines in a suitable range of power, based on Yamaha (2017). These have been deemed significant for the present application, due to the fact that power levels of interest here are much lower than those typical to usual ICE power plants

for aircraft, and the technical characteristics of these engines, built for prolonged use at constant speed and torque very close to a design point, are well suited for the power supply role. Fig. 4 presents the points composing the database and a possible fitting curve, which appears to capture the physics of the ICE scaling process with good accuracy. The proposed analytic relationship considered for the fitting is

$$\begin{aligned} &\text{if} P_{ICE} \geq P_{ICE_{min,DB}}: W_{ICE} = \log(P_{ICE}) \\ &\text{if} P_{ICE} < P_{ICE_{min,DB}}: W_{ICE} = \left(\frac{P_{ICE}}{P_{ICE_{min,DB}}}\right) W_{ICE_{min,DB}} \end{aligned} \tag{11}$$

where a linear interpolation is applied between zero and the minimum values $P_{ICE_{min,DB}}$ and $W_{ICE_{min,DB}}$ in the database.

Including a new energy source in the design process allows the definition of a new measure of energy, obtained as a sum of the electric energy in the battery E^*_{bat}, corresponding to the weight of the battery W^*_{bat}, and the chemical energy E_f stored in the available fuel W_f, as

$$E_0 = E^*_{bat} + E_f \tag{12}$$

where the energy term related to fuel can be expressed as $E_f = \frac{W_f e_f}{g}$, with e_f providing a measure of the specific energy of fuel.

For an assigned value of W^*_{bat} and P_{ICE} it is possible to compute cruising range R with a numerical procedure, accounting for the fact that the overall weight of the aircraft $W = W(t)$ will be varying during the cruise, differently from the purely electric case. This in turn implies that power required will be a function of time due to the component bound to lift, yielding

$$P_r^{cruise} = \frac{1}{2}\rho^{cruise}(V^{cruise})^3 S\, C_{D0} + \frac{k\, W(t)^2}{\frac{1}{2}\rho^{cruise} V^{cruise} S} \tag{13}$$

The chance to regulate the energy flow from the ICE to the battery in a series hybrid powertrain, hence in turn assigning $W = W(t)$, opens up the problem of power management. The effect on flight mechanics performance of the selected ICE power (and weight) time profile can be significant. Being not the focus of this study, we concentrate on a basic power management strategy, where the ICE is activated at the beginning of the cruise and kept operating at constant power. This results in a $W(t)$ linearly decreasing in time.

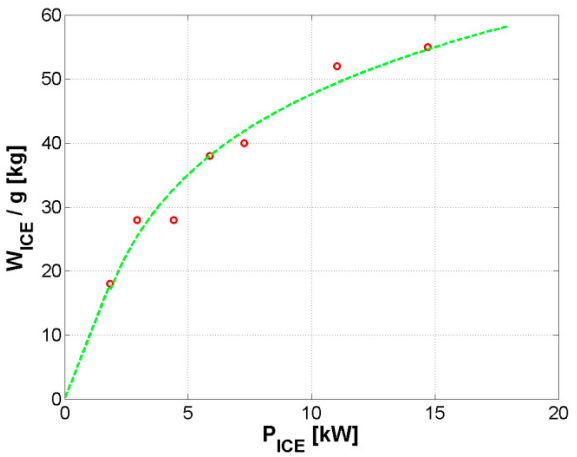

Fig. 4. Database and analytical fitting of ICE power plants for a hybrid electric propulsion system.

The value of P_{ICE} is henceforth kept constant, which greatly simplifies the ICE design and reduces cost. The design value of P_{ICE} can be set in proportion to a constant part of the power required for cruise P_r^{cruise}, defined here for convenience as $P_{r,C_{D0}}^{cruise}$, *i.e.* the power component bound to parasite drag, yielding

$$P_{ICE} = K_h \frac{1}{2}\rho^{cruise}(V^{cruise})^3 S\, C_{D0} = K_h\, P_{r,C_{D0}}^{cruise} \tag{14}$$

which is not a function of time. The coefficient K_h in Eq. 14 is a free parameter in the design process. Considering this variable instead of using power directly provides a better sensitivity with respect to the flight mechanics characteristics of the aircraft.

Now, considering all assumptions, for an assigned value of W_{bat}^{cruise}, considered equal to the value obtained from the purely electric design, for every couple of W_f and K_h it is possible to compute range R for a series hybrid aircraft as follows.

From P_{ICE} the weight W_{ICE} can be preliminarily computed from Eq. 11, and by Eq. 10 it is possible to find W^*_{bat}. The total weight W_{to}, which for the electric aircraft was a constant over time, can be assigned as the initial weight of the aircraft, *i.e.* at the beginning of the cruise when time $t = t_{in}$, $W(t = t_{in}) = W_{to}$. Similarly, from Eq. 12 it is possible to compute the initial value of energy $E_0(t = t_{in})$.

An integration in time can be run starting from the initial condition, computing for each time instant the battery energy flow $\dot{E}_{bat}(t) = P_{ICE}\eta_C - \frac{P_r^{cruise}(t)}{\eta_p}$, where η_C is a conversion efficiency in the battery recharge process. The weight flow $\dot{W} = -c_P P_{ICE}$ is a constant for the case of the power management profile considered here. It is noteworthy that the value of the brake specific fuel consumption c_P can be written as a function of the energy density of fuel e_f previously introduced and of the conversion efficiency of the ICE η_{ICE}, as $c_P = \frac{e_f \eta_{ICE}}{g}$.

From the flows of energy and weight it is possible to incrementally update the value of the aircraft weight, battery energy and overall energy level as

$$\begin{aligned} W(t+\Delta t) &= W(t) + \dot{W}\Delta t \\ E_{bat}(t+\Delta t) &= E_{bat}(t) + \dot{E}_{bat}(t)\Delta t \\ E_0(t+\Delta t) &= E_0(t) + \left(\dot{E}_{bat}(t) + \dot{W}\frac{e_f}{g}\right)\Delta t \end{aligned} \tag{15}$$

The integration in Eq. 15 is carried on until a termination condition is reached. A hierarchy of two conditions has been considered. The primary condition is $E_0 \geq 0$, implying that the cruise is over when electrical and fuel energy are over. The secondary condition is $E_{bat} \geq 0$, which stops the cruise if the energy in the battery reaches zero, which for a series hybrid with the assumed power management profile means that the electric motor cannot be powered any more.

Results of the application of this procedure to the considered motor-glider will be presented in the next section. From a design viewpoint, this procedure allows to drive two considerations that can be anticipated now. Firstly, the same range can be obtained for several choices of W_f and K_h. Secondarily, an optimal sizing curve on the W_f vs. K_h plane can be evidenced, allowing to choose the appropriate ICE engine power and fuel load to cover the desired range. Results on this study will be proposed in the last part of the following section.

5. Application studies

In a first stage the results obtained in Riboldi and Gualdoni (2016) for the case of a purely electric motor-glider will be recalled and commented. Subsequently, the analysis will be extended to the case of a hybrid-electric version of the same aircraft, according to the procedure introduced in Section 4.

5.1. Sizing of a small pure-electric aircraft

In order to complete the sizing procedure, it is necessary to assign some specifications and some aerodynamic characteristics. The latter can be guessed from the well-proven methods of Roskam(2003) for the preliminary design. Tables 1 and 2 show the desired performance of the considered motor-glider and the coefficients of the polar curves considered in the various phases of the design.

Table 1. Specifications for sizing matrix plot.

Specification	Value
$V_{stall}^{landing}$	40kn
$L^{take-off}$	200 m
$h^{airfield}$	3,000 m
h^{cruise}	3,000 m
V^{cruise}	90 m
h^{loiter}	3,000 m
V^{loiter}	0.9 V^{cruise}
V_v	400ft/min
V^{climb}	1.2V^{stall}
ξ	0.98
η_p	0.85

As can be seen from Table 1, an efficiency η_P of the propeller has been taken into account. The corresponding value is relatively high, but the power loss coefficient, also specified in Table 1, refers mainly to the decrease in propeller performance

due to operation at an off-design altitude. Actually no change in the performance of the electric motor is expected with altitude, differently from an ICE, especially for the small change in altitude expected in the considered design.

Table 2. Coefficients of polar curves.

Coefficient	Cruise value	Take-off value	Landing value
C_{D0}	0.0110	0.0310	0.1010
$C_{L,max}$	1.5	1.5	2.2
e	0.83	0.83	0.75

The resulting SMP was shown in Fig. 2, and is proposed again here with a focus on the most stringent requirements, forming the boundary of the space of solutions. An area of interest for the design solution corresponds to the region with the highest values of power and wing loading, meaning for a given take-off weight respectively the lowest possible engine power, yielding a low motor weight and cost, and the lowest wing area, meaning a smaller aircraft with less material to be used and consequently a lower production cost. Placing the design point on the limit is not indicated at this stage of the design where many hypothetical values are assumed and inaccuracies are presumably high. For this reason the design point, represented by the blue star, has been placed at a distance from the boundary, as shown in Fig. 5.

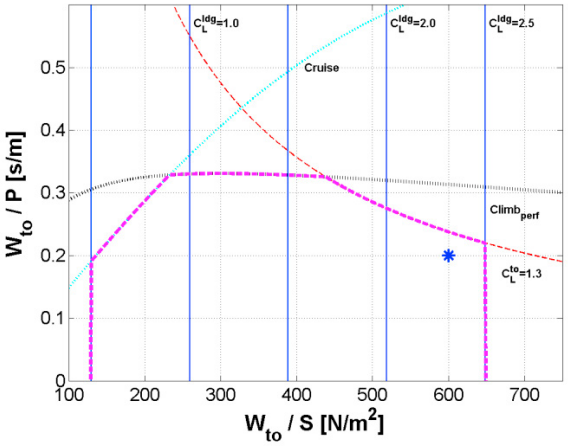

Fig. 5. Sizing matrix plot with selection of the design point.

After selecting the design point in terms of $\frac{W_{to}}{S}$ and $\frac{W_{to}}{P_{req}}$, it is possible to run the weight sizing procedure explained in Section 3. For running all the computations based on the mission profile it is necessary to add the data in Table 3, which are not necessary for computing the SMP.

Table 3. Mission profile requirements.

Performance item	Value
R	300 km
T^{loiter}	15 min
W_{pl}	150kg$_f$

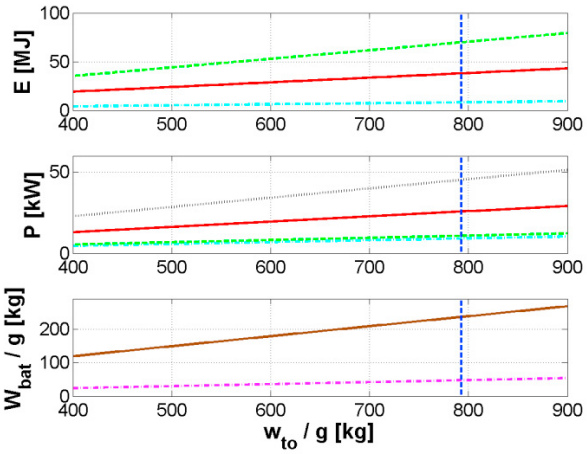

Fig. 6. Battery energy, power and weight as functions of W_{to}.

Figure 6 shows the effect of W_{to} on required battery power, energy and weight W_{bat}. On the two upper plots, the red solid, green dashed and cyan dash-dotted lines refer to climb, cruise and loiter respectively, whereas the black dotted line represent the constraint from the SMP on $\frac{W_{to}}{\frac{W_{to}}{P}}$. The dashed blue vertical line is placed at the design W_{to}. For the present design, it is clear from the two top plots that the cruise phase is the most demanding in terms of energy, whereas the most stringent power constraint is a result of the choice of the design point on the SMP, in turn due to take-off performance. In any case, from the third plot it is evident that the most imposing limit on battery weight comes from energy storage and not from battery power. This is clearly bound to the characteristics of the considered design, and these results may change significantly for aircraft intended for different missions.

Table 4 shows the final breakdown of the weights, obtained from the procedure summarized in Fig. 3. It should be noted that the value of the motor weight W_m has been hypothesized to be an assigned function of the required motor power (Riboldi and Gualdoni, 2016). The analytic relationship between the values of weight and power of the electric motor has been hypothesized based on a database of electric motors already installed on existing electric aircraft.

Table 4. Weight breakdown, power and energy required.

Specification	Value
W_{to}	793 kg_f
W_e	379 kg_f
W_m	23 kg_f
W_{bat}	241 kg_f
W_{pl}	150 kg_f
P_{req}/η_P	45.3 kW
E_{req}/η_P	116.1 MJ

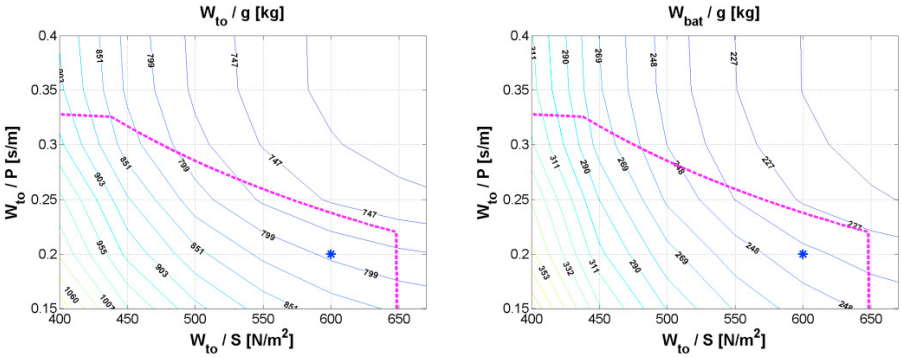

Fig. 7. Effect of a change in the design point on weights.

After clarifying the sizing procedure for the case of a specific design point on the SMP, it is interesting to check the sensitivity of some parameters to a change in the choice of the design point. Figure 7 shows the effect on W_{to} (left) and W_{bat} (right) for all couples of $\frac{W_{to}}{S}$ and $\frac{W_{to}}{P_{req}}$. As expected, the value of both weights is reduced in the top-right part of the space of solutions complying with the constraints, thus supporting the criterion for the choice of the design point introduced above. On the other hand, for the particular design of the motor-glider considered here, it can be seen that the gradient of the considered weights is rather mild for large ranges of $\frac{W_{to}}{S}$ and $\frac{W_{to}}{P_{req}}$, indicating that the choice of the design point is not critical.

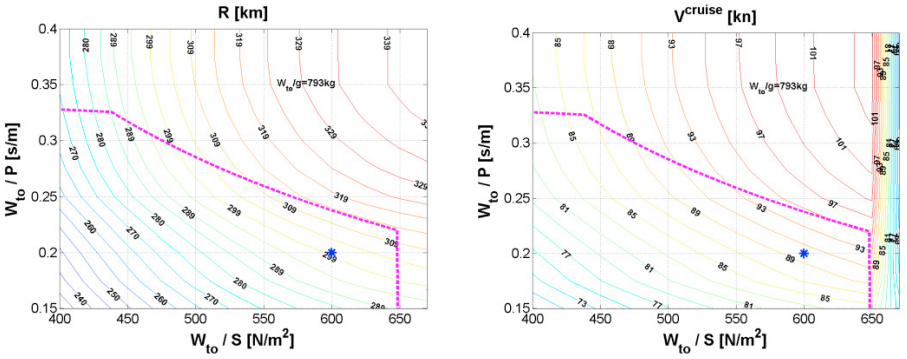

Fig. 8. Effects of a change in the design point on performance (fixed weights).

Further information about the quality of the solution come from a parameterized analysis where weight and its components are kept constant to the obtained design values, and some required performance of interest is changed. Figure 8 shows the result of such analysis for the case of the motor-glider, considering range (left) and cruising speed (right) as changing performance parameters. Once again, these result show that a change in the requirements aimed at increasing range or cruising speed would drive the solution towards higher wing and power loading. Even considering these metrics, it is possible to say that the top-right part of the envelope is the most attractive. Furthermore, it can be seen that both range and cruising speed show a gradient of relevant intensity with respect to wing and power loading.

5.2. Hybrid propulsion: trade-off analysis

The effect of the inclusion of an ICE to support the electrical power plant of the aircraft was carried out for the case of the motor-glider. With respect to the selected value of battery weight W_{bat}, the fraction pertaining to cruise W_{bat}^{cruise}= 142 kg was computed from the mission profile. Based on the polar in clean configuration, the reference value of required power for the ICE could be computed as $\frac{P_{r,C_{D0}}^{cruise}}{\eta_p}$= 7.48 kW, corresponding to the part of required power not depending on current weight.

In order to run the analysis presented in Section 4 it is necessary to specify the values of some energy-related quantities. The considered fuel energy density has been assumed as e_f= 45 MJ/kg, a typical value for hydrocarbon fuels. The conversion efficiency of the ICE can be assumed as η_E= 0.35, whereas the efficiency of the battery recharge process has been set to η_C= 0.85. This implies an overall efficiency of the transformation of the energy stored as fuel into battery energy slightly under 30%.

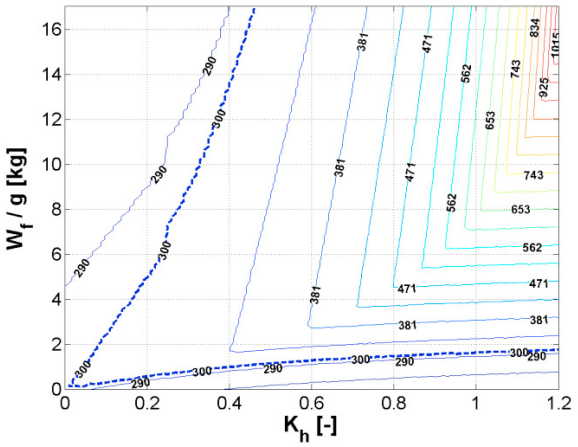

Fig. 9. Contour plot of cruising range as a function of W_f and K_h.

As seen in Section 4, the fuel weight W_f and the power of the ICE system, represented by K_h, have been considered to characterize the behaviour of cruising range R. In particular, R was computed for each couple of values. The result is presented in Fig. 9. Considering the line corresponding to R = 300 km, which is the design range for the purely electric case – the thicker line in Fig. 9 – it is possible to notice that the space of solutions can be divided into three main regions.

For low values of K_h, meaning lower ICE engine power P_{ICE}, and higher values of W_f, the range is reduced with respect to that obtained with purely electric propulsion. This corresponds to an ICE which is underpowered with respect to the fuel loaded on the aircraft, so that fuel is burnt at too slow a rate and the battery is totally discharged before fuel is over – which is a termination condition for range computation, as explained in Section 4. On the other end, for low values of the weight W^*_{bat} and especially for higher K_h the result is a similarly reduced level of performance with respect to the electric design. In this case, the reason is the low fuel embarked, which is burnt at an excessive rate, so that for a final part of the cruise the only energy on board is that in the battery, as for the case of a purely electric design, but the weight of the aircraft is higher due to the presence of the ICE plant, thus reducing actual range. The third and wider area corresponds to higher range values with respect to what is obtained with purely electric propulsion. As a general comment, the increase in range is considerable also for a small amount of stored fuel and a low-power ICE. This highlights once again that the energy density of the batteries is the most relevant limit of purely electric propulsion systems, whereas fossil fuels benefit from much more favorable values. The angularity in the curves corresponds to a condition where the cruise ends at the same time as the fuel reserve is emptied. The envelope of these conditions constitutes an optimum for the design.

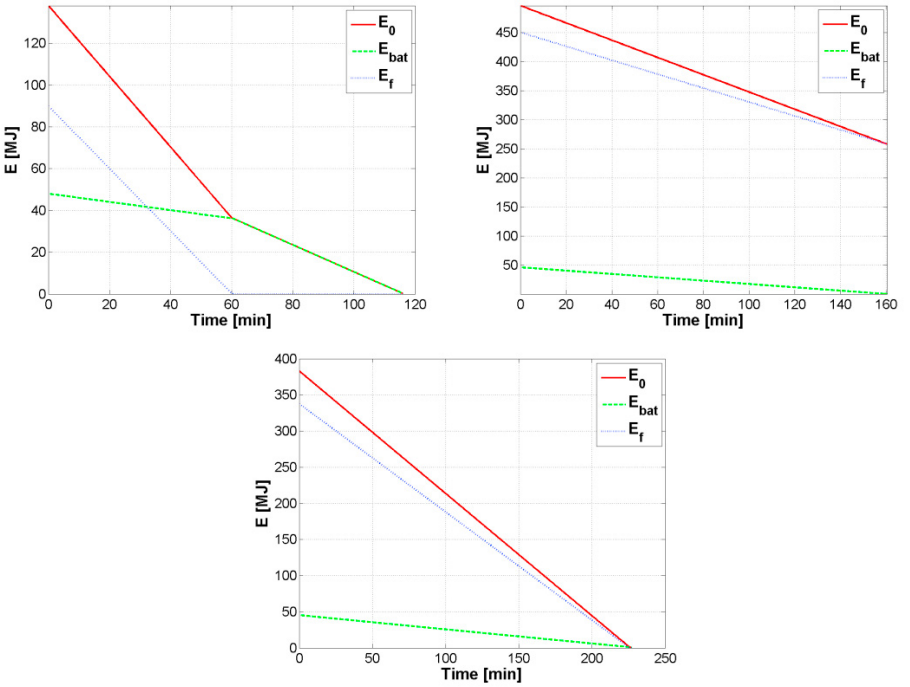

Fig. 10. Examples of time histories of total energy, battery energy and fuel energy, for three different design points. Top plots: non-optimal conditions, low (left) and high initial fuel energy level (right). Bottom plot: optimal condition.

To better highlight the differences in the presented scenarios, three example time histories of total energy and its components are presented in Fig. 10. The top left and top right plots correspond to non-optimal design conditions, where the energy stored as fuel is lower (left) or higher (right) than optimal. The corresponding design points on Figure 9 are located at K_h = 0.8 and W_f/g = 10 kg for the former case, and at K_h = 1.0 and W_f/g = 2 kg for the latter. In the former case all fuel is burned in a first stage of the cruise, leaving the electric motor and batteries to cover all the power and energy demand for the rest of the cruise. In the latter scenario fuel is burned at a low rate, and batteries get totally discharged before all fuel has been burned. As previously explained, being an unfeasible working condition for a series hybrid, the cruise is interrupted correspondingly.

The bottom plot on Fig. 10, corresponding to a design point where K_h = 1.0 and W_f/g = 7.67 kg, represents an optimized condition, where both energy components reach zero at the same time. It is noteworthy that the duration of the cruise phase in both non-optimal cases is lower than for the optimized case. This duration can be translated directly into range, based on the adopted assumption of constant cruising speed.

From Fig. 10 it is also possible to appreciate how the total energy level at the beginning of the cruise can be altered significantly by slight changes in the quantity of fuel on board, like those considered in this work. Furthermore, the energy stored in the batteries is almost unaffected by the limited change in the battery weight considered here. These effects are clearly a result of the higher energy density of hydrocarbon fuels with respect to that of batteries at the current level of technology.

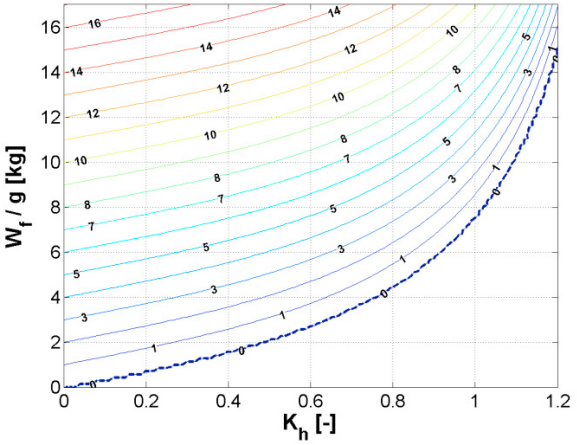

Fig. 11. Contour plot of residual fuel weight at the end of the cruise as a function ofW_f and K_h.

A contour plot of the residual fuel weight at the end of the cruise is presented in Fig. 11. For each installed power – *i.e.*K_h – for increasing values of fuel weight W_f the maximum attainable range is obtained for a residual fuel weight equal to zero. For the same value of K_h, a value of W_f below the optimum corresponds to an overpowered ICE and insufficient fuel, whereas a value of W_f above the optimum reflects an excessive fuel load for the assigned ICE power.

6. Conclusion

A procedure for the preliminary weight sizing of light electric aircraft has been illustrated. It is mainly based on the integrated use of a statistical regression of data from existing models, a suitable definition of the breakdown of the take-off weight, and the sizing matrix represented in the SMP. For the case of electric aircraft, where the definition of fuel fractions typical to ICE-powered aircraft cannot be applied, these ingredients allow to build a quick procedure for preliminary sizing similar to more classical methods. The validity of the procedure has been demonstrated through the preliminary sizing of a motor-glider.

In a second stage, the procedure for the sizing of purely electric aircraft has been extended to analyze the effects of the inclusion of an ICE in a series-hybrid configuration. To the aim of highlighting the advantages of the adoption of this powertrain architecture with respect to a purely electric one, specific constraints have been placed on the weights of the ICE engine, ensuring a fair trade-off comparison with respect to the purely electric case. Considering the cruise phase and the adopted example design, it can be seen that the series-hybrid configuration is generally advantageous, and also that an optimum of the powertrain design can be found in terms of weight of fuel and ICE power.

References

Cao, W., Mecrow, B., Atkinson, G., Bennett, J., Atkinson, D., 2012. Overview of Electric Motor Technologies Used for More Electric Aircraft (MEA). IEEE Transactions on Industrial Electronics 59.9, 3523–3531.

Choi, T., Soban, D., Mavris, D., 2005. Creation of a Design Framework for All-Electric Aircraft Propulsion Architectures, 3rd International Energy Conversion Engineering Conference, San Francisco, USA.

Cohen,J. P., Coughlin, C. C., 2008. Spatial Hedonic Models of Airport Noise; Proximity and Housing Prices. Journal of Regional Science 48,859–878 .

Kromer, M., Heywood, J., 2007. Electric Powertrains: Opportunities and Challenges in the U.S. Light-Duty Vehicle Fleet. Sloan Automotive Laboratory, Massachusetts Institute of Technology, Cambridge.

Miljkovic, D.,Ivosevic,J.,Bucak, T., 2013. Psycho-Acoustical Ergonomics in a Light Aircraft Interior,5th International Conference Ergonomics, Zadar, Croatia.

Morrell, P., Lu, C., 2000. Aircraft Noise Social Cost and Charge Mechanisms - A Case Study of Amsterdam Airport Schiphol. Transportation Research Part D 5.4, 305–320.

Ozawa, K., 2009. Lithium-ion Rechargeable Batteries. Wiley-VCH.

Pistoia, G., 2010. Electric and Hybrid Vehicles. Elsevier.

Pornet, C.,Gologan, C.,Vratny, P., Seitz, A., Schmitz, O.,Isikveren, A.,Hornung, M., 2015. Methodology for Sizing and Performance Assessment of Hybrid Energy Aircraft. Journal of Aircraft 52.1, 341–352.

Pornet, C., Kaiser, S.,Isikveren, A.,Hornung, M., 2014. Integrated Fuel–Battery Hybrid for a Narrow-Body Sized Transport Aircraft. Aircraft Engineering and Aerospace Technology 86.6, 568–574.

Raymer, D., 2012. Aircraft Design: A Conceptual Approach. AIAA Education Series.

Riboldi, C., Gualdoni, F., 2016. An Integrated Approach to the Preliminary Weight Sizing of Small Electric Aircraft. Aerospace Science and Technology 58, 134–149.

Roskam, J., 2003. Airplane Design: Part I-VII. DAR Corporation.

Yamaha Motor Corporation, 2017. Boat Motor; Portable Outboard.